Editors' Suggestion

Observation of a Lee-Huang-Yang Fluid

Thomas G. Skov, Magnus G. Skou, Nils B. Jørgensen, and Jan J. Arlt
Center for Complex Quantum Systems, Department of Physics and Astronomy, Aarhus University, Ny Munkegade 120, DK-8000 Aarhus C, Denmark

(Received 6 November 2020; revised 19 April 2021; accepted 18 May 2021; published 11 June 2021)

We observe monopole oscillations in a mixture of Bose-Einstein condensates, where the usually dominant mean-field interactions are canceled. In this case, the system is governed by the next-order Lee-Huang-Yang (LHY) correction to the ground state energy, which describes the effect of quantum fluctuations. Experimentally such a LHY fluid is realized by controlling the atom numbers and interaction strengths in a ^{39}K spin mixture confined in a spherical trap potential. We measure the monopole oscillation frequency as a function of the LHY interaction strength as proposed recently by Jrgensen *et al.* [Phys. Rev. Lett. **121**, 173403 (2018)] and find excellent agreement with simulations of the complete experiment including the excitation procedure and inelastic losses. This confirms that the system and its collective behavior are initially dominated by LHY interactions. Moreover, the monopole oscillation frequency is found to be stable against variations of the involved scattering lengths in a broad region around the ideal values, confirming the stabilizing effect of the LHY interaction. These results pave the way for using the nonlinearity provided by the LHY term in quantum simulation experiments and for investigations beyond the LHY regime.

DOI: 10.1103/PhysRevLett.126.230404

The advent of well-controlled mixtures of quantum gases with tunable interaction strengths has enabled fascinating insights beyond the mean-field description of such systems. This is particularly important for strongly interacting systems of current interest, where the mean-field description typically breaks down as higher-order effects become important. Most prominently, the next-order Lee-Huang-Yang (LHY) correction describes the effect of quantum fluctuations on the ground state energy of a bosonic quantum gas [1], and its effect has been observed in several experiments [2–6], emphasizing its importance in describing systems beyond the mean-field regime.

The ability to tune the interaction strength is especially useful in cases with competing interactions, such as two-component quantum mixtures in which both inter- and intracomponent interactions are relevant. Here, the LHY contribution to the energy functional has been extended to the case of homonuclear bosonic mixtures [7] and recently an effective expression was derived for the heteronuclear case [8]. In particular, the influence of LHY physics can be observed more readily by tuning the interactions such that other contributions to the energy density are suppressed. This approach enables the formation of self-bound droplets stabilized by the repulsive LHY energy contribution [9], which have been observed and investigated in homonuclear [10–13] and heteronuclear [14] bosonic mixtures. Similar observations have been made in dipolar quantum gases [15–18], culminating in the observation of supersolid behavior in these systems [19–21].

Here, we consider a quantum mixture in which the mean-field interactions cancel exactly such that interactions in the mixture are governed primarily by the LHY correction [22]. In practice, this can be achieved utilizing a two-component Bose-Einstein condensate (BEC) characterized by scattering lengths a_{ij} between components i and j. For scattering lengths $\delta a = a_{12} + \sqrt{a_{11}a_{22}} = 0$ and densities $n_2/n_1 = \sqrt{a_{11}/a_{22}}$, the mean-field contributions to the energy functional vanish, and the resulting LHY fluid can be characterized by measuring its monopole oscillation frequency, which differs significantly from that of a single-component BEC [22].

In this Letter we experimentally investigate the collective excitations of such a LHY fluid in a ^{39}K spin mixture. We measure the monopole oscillation frequency depending on the strength of the LHY interaction and its magnetic field dependence in the vicinity of the $\delta a = 0$. To evaluate the results, we perform detailed simulations of the system including the effect of inelastic losses and the preparation sequence of the mixture. Throughout the investigated region we find good agreement between experimental observations and theory, demonstrating a detailed understanding of the LHY fluid.

To realize a LHY fluid experimentally, we employ the $|F = 1, m_F = -1\rangle \equiv |1\rangle$ and $|F = 1, m_F = 0\rangle \equiv |2\rangle$ states of the lowest hyperfine manifold of ^{39}K, which offer favorable Feshbach resonances for realizing $\delta a = 0$ [9–11,22]. Based on models for the scattering lengths presented in Refs. [12,23,24] we find that the system

 © 2021 American Physical Society

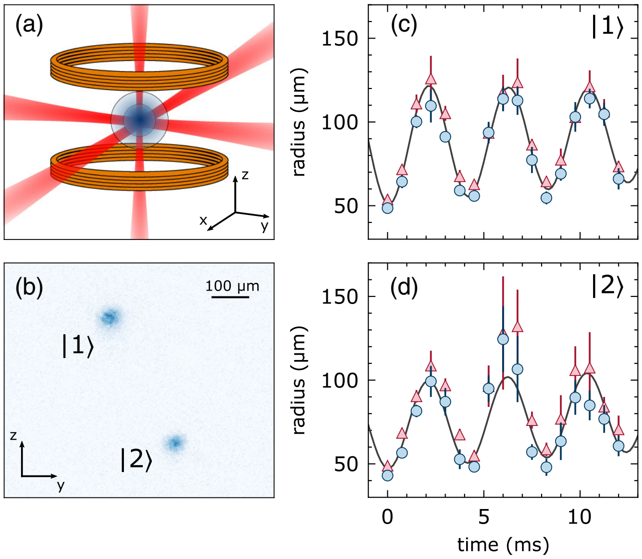

FIG. 1. (a) Schematic representation of the experiment showing a LHY fluid undergoing monopole oscillations in a spherical potential composed of three red-detuned laser beams. (b) Typical absorption image after time of flight (TOF) during which atoms in states $|1\rangle$ and $|2\rangle$ are separated by a magnetic field gradient. (c), (d) Extracted BEC radii of atoms in states $|1\rangle$ (c) and $|2\rangle$ (d) after 28 ms TOF as a function of evolution time. The radii along the y and z directions are shown as blue dots and red triangles, respectively, and the gray lines are fits of Eq. (1) to the mean radius. The data were recorded for $\omega_0 = 2\pi \times 113.1(6)$ Hz and $N = 2.3(3) \times 10^4$ corresponding to $U = 0.5(1)$.

fulfills $\delta a = 0.0(3)\ a_0$ at 56.83(2) G with $a_{11} = 33.3(3)\ a_0$, $a_{22} = 84.2(3)\ a_0$, and $a_{12} = -52.97(1)\ a_0$, where a_0 is the Bohr radius. Given these scattering lengths, the requirement for the relative densities is $n_2/n_1 = 0.629(3)$ corresponding to ~40% of the total atom number in the $|2\rangle$ state.

In practice, the experiment starts from a nearly pure BEC in the $|1\rangle$ state [25] trapped in a spherically symmetric harmonic potential. The employed optical dipole trap (ODT) is composed of a beam along each Cartesian axis [Fig. 1(a)], allowing the realization of almost identical trap frequencies ω_0 in all directions. The initial BEC in the $|1\rangle$ state is prepared at the target magnetic field in the vicinity of $\delta a = 0$. Subsequently, the measurement is initialized by transferring part of the atoms to the $|2\rangle$ state using a radio-frequency (rf) pulse tuned to the bare atomic transition. Because of the sudden change in the interaction strengths, the system starts to contract and strong monopole oscillations are initialized. This preparation method is necessary because inelastic losses of atoms in the $|2\rangle$ state limit the lifetime of the mixture [10–13]. Afterwards, the mixture is held for a variable evolution time before release from the trap and subsequent absorption imaging. During time of flight (TOF), the states are separated by applying a magnetic field gradient, which enables the resulting cloud profiles to be evaluated separately [Fig. 1(b)]. Note that imaging the clouds after TOF results in a phase shift of π compared to the in-trap oscillations since the momentum distribution is observed.

For each evolution time, the cloud profiles are fitted using a Thomas-Fermi profile and the cloud radii along the y and z directions are extracted. An example of such a measurement is shown in Figs. 1(c) and 1(d), where the cloud radii feature large amplitude oscillations as a consequence of the experimental preparation method. For both states, the y and z radii oscillate in phase, confirming that the oscillations are monopolar. Moreover, the two clouds initially oscillate jointly as expected for a LHY fluid, which can be described in a one-component framework [22]. With increasing evolution time, however, inelastic losses of atoms in the $|2\rangle$ state result in the appearance of small phase differences and deviations from pure sinusoidal behavior. Because of these losses, we use the radius of the cloud in the $|1\rangle$ state for the further evaluation because it provides more reliable results.

The large oscillation amplitude and inelastic losses require a detailed theoretical analysis, and we simulate the experiment [26,27] using two coupled Gross-Pitaevskii equations including the LHY contributions [7,9]. We first calculate the ground state of a pure BEC in the $|1\rangle$ state at the target magnetic field. The fast transfer is then modeled by assuming that both components start in the calculated ground state wave function, but with properly adjusted atom numbers and scattering lengths. In agreement with experiment, this results in monopole oscillations of large amplitude. Inelastic losses due to three-body recombination are included using imaginary terms corresponding to the relevant loss channels (Supplemental Material [28]).

This simulation allows us to quantify the monopole oscillation frequency as a function of the dimensionless parameter $U = N^{3/2}|a_{12}/a_{\mathrm{ho}}|^{5/2}$ with total atom number N, harmonic oscillator length $a_{\mathrm{ho}} = \sqrt{\hbar/m\omega_0}$, and mass m. This parameter corresponds to the ratio of the LHY interaction energy to the kinetic energy and thus characterizes the interaction strength of the LHY fluid [22]. Figure 2(a) shows simulated cloud radii for $U = 1.2$ including inelastic losses based on the three-body loss coefficients given in Refs. [11,12]. Similar to the experiment, the two components initially contract and start to oscillate jointly. As the density increases, the losses in the $|2\rangle$ state set in, resulting in a cascading loss of atoms coinciding with the minima of the radii [Fig. 2(b)], leading to a decay of the oscillations. Because the losses primarily affect atoms in the $|2\rangle$ state, the system is displaced away from the ideal density ratio $n_2/n_1 = \sqrt{a_{11}/a_{22}}$, resulting in increasing mean-field interactions. This leads to an additional repulsion of atoms in the $|1\rangle$ state, which explains the increasing offset and amplitude visible in their cloud radius. As a consequence, the resulting oscillation is determined both by the initial evolution, governed by the dominant LHY correction, and the later evolution, where the mean-field contributions become relevant and the system deviates from a pure LHY fluid.

To capture these effects, we fit a model function to the simulated radius r as a function of evolution time t,

$$r(t) = r_0 + st + A\sin(\omega t + \phi)\exp(-t/\tau). \quad (1)$$

Here, r_0 is an offset radius, s is the slope, A is the oscillation amplitude, ω is the angular frequency, ϕ is a phase offset, and τ is the time constant describing the growth or decay of the oscillations. Note that a small frequency chirp could arise during the evolution time due to the increasing mean field interactions. In our simulations, however, we do not observe a significant chirp and therefore neglect it. As a result, the extracted frequency ω describes the average oscillation frequency within the data range. Even though the simulated radius deviates from a regular sinusoidal in its extrema as shown in Fig. 2(a), Eq. (1) captures the oscillation frequency well.

Figure 2(c) shows the simulated monopole oscillation frequency of atoms in the $|1\rangle$ state as a function of the LHY interaction strength, with and without inelastic losses. For comparison, the oscillation frequency of the LHY fluid in the low-amplitude limit [22] and the noninteracting limit are shown. For low interaction strengths, all results including the LHY correction follow a common rising trend; however, our simulations quickly deviate from the low-amplitude result showing a pronounced reduction in frequency as a consequence of the large oscillation amplitudes. Furthermore, the effect of inelastic losses becomes apparent as an additional decrease of the oscillation frequency, settling at $\omega/\omega_0 \sim 2.18$ for the investigated trap [35]. Comparing the simulated results to the noninteracting limit, it is clear that the LHY correction has considerable influence on the oscillatory behavior, even under the influence of inelastic losses. Based on this thorough theoretical analysis, a comparison with our experimental results is now possible.

In a first set of experiments, we investigate the dependence of the monopole frequency on the LHY interaction strength. We follow the experimental procedure outlined above, preparing the initial BEC at the magnetic field corresponding to $\delta a = 0$ and initialize the mixture using a rf pulse of 1.3 μs duration, which realizes the required density ratio. This pulse length was chosen based on Rabi oscillation measurements using cold thermal clouds. To scan the LHY interaction strength, we adjust the total number of initial BEC atoms by varying the loading time of ^{39}K in the dual-species magneto-optical trap [25]. The resulting oscillations yield measurements similar to Figs. 1(c) and 1(d) and we extract the oscillation frequency by fitting Eq. (1) to the mean of the cloud radii in the y and z directions as a function of evolution time (Supplemental Material [28]).

Figure 3 shows experimental results for a range of trap frequencies together with the simulated results for $\omega_0 = 2\pi \times 113.6$ Hz also shown in Fig. 2. Because the

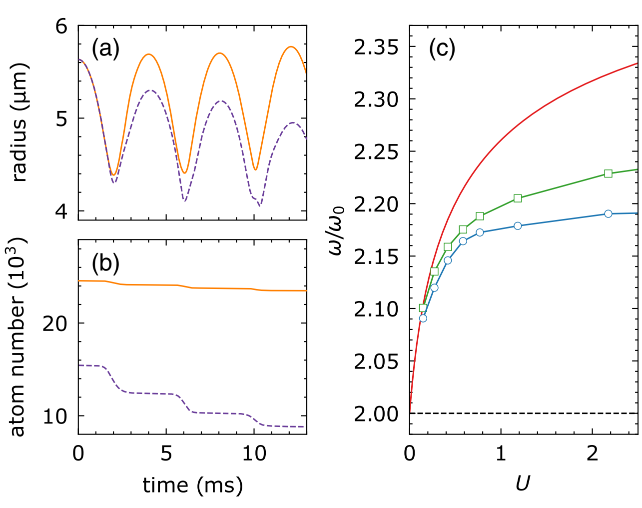

FIG. 2. Results of the dynamical two-component simulations. (a),(b) Simulated radii and atom numbers for a LHY fluid including inelastic losses for $\omega_0 = 2\pi \times 113.6$ Hz and $N = 4 \times 10^4$ corresponding to $U = 1.2$. Results for atoms in states $|1\rangle$ and $|2\rangle$ are shown as solid orange and dashed purple lines, respectively. (c) Extracted oscillation frequencies of atoms in the $|1\rangle$ state as a function of LHY interaction strength. Results with and without inelastic losses are shown as blue circles and green squares, respectively. The low-amplitude limit is shown as a red line and the noninteracting limit is shown as a dashed black line.

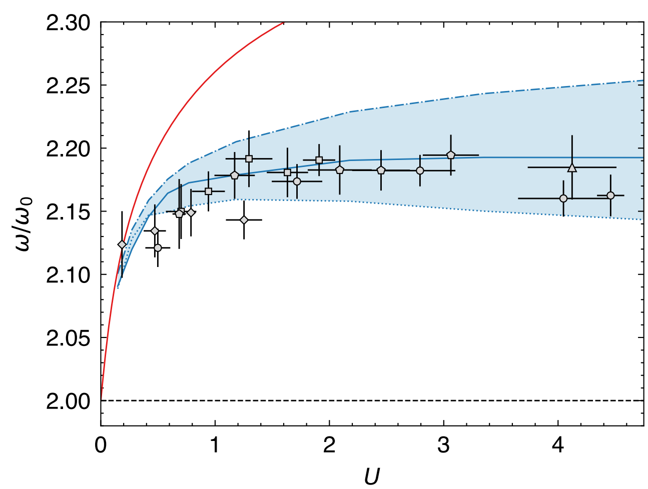

FIG. 3. Observed monopole oscillation frequency depending on interaction strength of the LHY fluid for spherical traps with $\omega_0 = 2\pi \times 113.1(6)$ Hz (circles), 113.7(1) Hz (squares), 115.3 (4) Hz (diamonds), 111.1(3) Hz (pentagons), and 110.9(5) Hz (triangles). Simulated results calculated for $\omega_0 = 2\pi \times 113.6$ Hz including inelastic losses are shown as a blue line. The dash-dotted and dotted lines correspond to simulations without losses and a doubled loss coefficient for the channel involving three atoms in the $|2\rangle$ state, respectively. The red line shows the monopole frequency of an ideal LHY fluid in the low-amplitude limit and the dashed black line shows the noninteracting limit.

exact loss coefficients are not well known, we include two limiting cases in our simulations: The upper limit of the light blue area shows simulated results neglecting losses entirely and the lower limit doubles the loss coefficient for the channel involving three atoms in the $|2\rangle$ state, corresponding to the upper limit given in Refs. [11,12]. For comparison, we again show the low-amplitude limit of a LHY fluid and the noninteracting limit. The experimentally obtained oscillation frequencies display a clear upward trend for $U \lesssim 1.5$ and for increasing interaction strengths, the oscillation frequency settles at a value determined by the LHY interactions, the large oscillation amplitudes, and inelastic losses. The overall agreement between theory and experiment is very good and we conclude that the mixture is indeed initially dominated by the LHY correction.

In a second set of experiments, we investigate the stability of the monopole frequency of the system against variations of the scattering lengths in the vicinity of $\delta a = 0$. The experiment is performed using a trap frequency $\omega_0 = 2\pi \times 110.9(5)$ Hz and atom number $N = 9.4(6) \times 10^4$ corresponding to $U = 4.1(4)$ for $\delta a = 0$. We vary the magnetic field at which the mixture is prepared, effectively varying δa, which is primarily influenced by a_{22}, as a_{11} and a_{12} are approximately constant within the investigated magnetic field range. Note that we keep the length of the rf pulse, which initializes the experiment, constant and hence the ideal density ratio, $n_2/n_1 = \sqrt{a_{11}/a_{22}}$ is only fulfilled initially at exactly $\delta a = 0$. Within the range of magnetic fields investigated, this corresponds to a minor relative deviation from the ideal ratio by $\pm 10\%$, which is included in the simulations.

Figure 4 shows experimentally observed and simulated monopole oscillation frequencies as a function of magnetic field and δa. When including the LHY correction, the simulated oscillation frequency decreases slowly with decreasing magnetic field. On the contrary, omitting the LHY correction results in a rapid decrease of the oscillation frequency toward the noninteracting limit of $\omega/\omega_0 = 2$ when approaching $\delta a = 0$. Beyond this point, the system collapses without the repulsive energy contribution from the LHY correction.

For $\delta a \gtrsim 0$ the experimental results agree very well with the simulation including the LHY correction. For negative δa the agreement is less good, which we attribute to the sensitivity of the simulation to the exact loss coefficients for increasingly attractive mean-field interactions. Here, the losses almost completely remove the population in state $|2\rangle$, which reduces the validity of our simulation. Nonetheless, the experimental data show that the LHY correction vastly influences the monopole oscillation frequency in a region around $\delta a = 0$ and prevents the collapse of the mixture for attractive mean-field interactions. This agrees with the theoretical results of Jørgensen *et al.* [22], who found that the LHY energy dominates the interactions within a window around the ideal magnetic field. Note that droplet formation in the regime $\delta a < 0$ is contained in our theoretical analysis; however, our experimental atom number ratios are unfavorable for the observation of droplets.

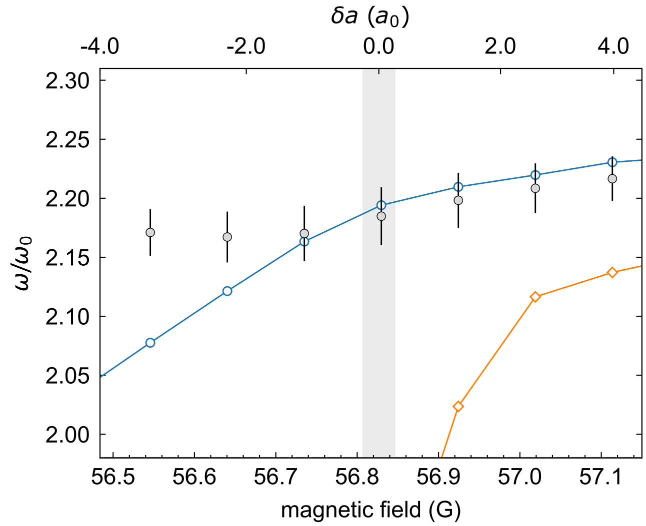

FIG. 4. Monopole frequency of the spin mixture depending on magnetic field and δa. Experimental results for $\omega_0 = 2\pi \times 110.9(5)$ Hz and $N = 9.4(6) \times 10^4$ corresponding to $U = 4.1(4)$ are shown as gray points. Simulated results using the same parameters with and without including the LHY correction are shown as blue circles and orange diamonds, respectively. The shaded region indicates the magnetic field regime where $\delta a = 0$ within 1σ. The horizontal errors on the experimental results are smaller than the markers.

In conclusion, we have experimentally realized a LHY fluid and investigated its monopole oscillation frequency depending on the LHY interaction strength, finding excellent agreement with detailed simulations taking the experimental preparation method and inelastic losses into account. Our experimental results show that the monopole frequency of the system is stable against variations of the involved scattering lengths, displaying a large stability region around $\delta a = 0$, where the repulsive LHY interaction prevents collapse of the mixture.

These results pave the way for further investigations of the LHY dominated regime with interesting research directions including higher-order collective modes and different trap geometries. Furthermore, the LHY fluid provides a promising platform for observing even higher-order effects such as the next-order correction to the energy of a Bose gas, E_{WHPS} [36,37]. On a broader scale, the realization of a LHY fluid enables new quantum simulation experiments utilizing the quartic nonlinearity, which governs the interactions of the system. Such experiments would ideally be realized in a system suffering less severely from inelastic losses than the ^{39}K spin mixture considered here. Building on the results of Minardi *et al.* [8], a promising candidate for such experiments could therefore be the ^{41}K-^{87}Rb mixture, which was recently found to support the existence of long-lived quantum droplets [14].

We acknowledge support from the Villum Foundation, the Carlsberg Foundation, the Independent Research Fund Denmark, and the Danish National Research Foundation through the Center of Excellence "CCQ" (Grant Agreement No. DNRF156).

[1] T. D. Lee, K. Huang, and C. N. Yang, Phys. Rev. **106**, 1135 (1957).
[2] A. Altmeyer, S. Riedl, C. Kohstall, M. J. Wright, R. Geursen, M. Bartenstein, C. Chin, J. H. Denschlag, and R. Grimm, Phys. Rev. Lett. **98**, 040401 (2007).
[3] Y. I. Shin, A. Schirotzek, C. H. Schunck, and W. Ketterle, Phys. Rev. Lett. **101**, 070404 (2008).
[4] S. B. Papp, J. M. Pino, R. J. Wild, S. Ronen, C. E. Wieman, D. S. Jin, and E. A. Cornell, Phys. Rev. Lett. **101**, 135301 (2008).
[5] N. Navon, S. Nascimbène, F. Chevy, and C. Salomon, Science **328**, 729 (2010).
[6] N. Navon, S. Piatecki, K. Günter, B. Rem, T. C. Nguyen, F. Chevy, W. Krauth, and C. Salomon, Phys. Rev. Lett. **107**, 135301 (2011).
[7] D. M. Larsen, Ann. Phys. (N.Y.) **24**, 89 (1963).
[8] F. Minardi, F. Ancilotto, A. Burchianti, C. D'Errico, C. Fort, and M. Modugno, Phys. Rev. A **100**, 063636 (2019).
[9] D. S. Petrov, Phys. Rev. Lett. **115**, 155302 (2015).
[10] C. R. Cabrera, L. Tanzi, J. Sanz, B. Naylor, P. Thomas, P. Cheiney, and L. Tarruell, Science **359**, 301 (2018).
[11] G. Semeghini, G. Ferioli, L. Masi, C. Mazzinghi, L. Wolswijk, F. Minardi, M. Modugno, G. Modugno, M. Inguscio, and M. Fattori, Phys. Rev. Lett. **120**, 235301 (2018).
[12] P. Cheiney, C. R. Cabrera, J. Sanz, B. Naylor, L. Tanzi, and L. Tarruell, Phys. Rev. Lett. **120**, 135301 (2018).
[13] G. Ferioli, G. Semeghini, L. Masi, G. Giusti, G. Modugno, M. Inguscio, A. Gallemí, A. Recati, and M. Fattori, Phys. Rev. Lett. **122**, 090401 (2019).
[14] C. D'Errico, A. Burchianti, M. Prevedelli, L. Salasnich, F. Ancilotto, M. Modugno, F. Minardi, and C. Fort, Phys. Rev. Research **1**, 033155 (2019).
[15] H. Kadau, M. Schmitt, M. Wenzel, C. Wink, T. Maier, I. Ferrier-Barbut, and T. Pfau, Nature (London) **530**, 194 (2016).
[16] I. Ferrier-Barbut, H. Kadau, M. Schmitt, M. Wenzel, and T. Pfau, Phys. Rev. Lett. **116**, 215301 (2016).
[17] M. Schmitt, M. Wenzel, F. Böttcher, I. Ferrier-Barbut, and T. Pfau, Nature (London) **539**, 259 (2016).
[18] L. Chomaz, S. Baier, D. Petter, M. J. Mark, F. Wächtler, L. Santos, and F. Ferlaino, Phys. Rev. X **6**, 041039 (2016).
[19] F. Böttcher, J.-N. Schmidt, M. Wenzel, J. Hertkorn, M. Guo, T. Langen, and T. Pfau, Phys. Rev. X **9**, 011051 (2019).
[20] L. Chomaz, D. Petter, P. Ilzhöfer, G. Natale, A. Trautmann, C. Politi, G. Durastante, R. M. W. van Bijnen, A. Patscheider, M. Sohmen, M. J. Mark, and F. Ferlaino, Phys. Rev. X **9**, 021012 (2019).
[21] L. Tanzi, E. Lucioni, F. Famà, J. Catani, A. Fioretti, C. Gabbanini, R. N. Bisset, L. Santos, and G. Modugno, Phys. Rev. Lett. **122**, 130405 (2019).
[22] N. B. Jørgensen, G. M. Bruun, and J. J. Arlt, Phys. Rev. Lett. **121**, 173403 (2018).
[23] L. Tanzi, C. R. Cabrera, J. Sanz, P. Cheiney, M. Tomza, and L. Tarruell, Phys. Rev. A **98**, 062712 (2018).
[24] R. Chapurin, X. Xie, M. J. Van de Graaff, J. S. Popowski, J. P. D'Incao, P. S. Julienne, J. Ye, and E. A. Cornell, Phys. Rev. Lett. **123**, 233402 (2019).
[25] L. Wacker, N. B. Jørgensen, D. Birkmose, R. Horchani, W. Ertmer, C. Klempt, N. Winter, J. Sherson, and J. J. Arlt, Phys. Rev. A **92**, 053602 (2015).
[26] X. Antoine and R. Duboscq, Comput. Phys. Commun. **185**, 2969 (2014).
[27] X. Antoine and R. Duboscq, Comput. Phys. Commun. **193**, 95 (2015).
[28] See Supplemental Material at http://link.aps.org/supplemental/10.1103/PhysRevLett.126.230404 for further details, which includes Refs. [2,7,9,11–14,25–27,29–34].
[29] M. Scherer, B. Lücke, J. Peise, O. Topic, G. Gebreyesus, F. Deuretzbacher, W. Ertmer, L. Santos, C. Klempt, and J. J. Arlt, Phys. Rev. A **88**, 053624 (2013).
[30] D. Lobser, A. Barentine, E. Cornell, and H. Lewandowski, Nat. Phys. **11**, 1009 (2015).
[31] F. Ancilotto, M. Barranco, M. Guilleumas, and M. Pi, Phys. Rev. A **98**, 053623 (2018).
[32] H. Hu and X.-J. Liu, Phys. Rev. Lett. **125**, 195302 (2020).
[33] M. Zaccanti, B. Deissler, C. D'Errico, M. Fattori, M. Jona-Lasinio, S. Mller, G. Roati, M. Inguscio, and G. Modugno, Nat. Phys. **5**, 586 (2009).
[34] S. Lepoutre, L. Fouché, A. Boissé, G. Berthet, G. Salomon, A. Aspect, and T. Bourdel, Phys. Rev. A **94**, 053626 (2016).
[35] We have confirmed that varying the trap frequency in the range 111–118 Hz makes negligible difference in the extracted frequency.
[36] A. Fetter and J. Walecka, *Quantum Theory of Many-Particle Systems*, Dover Books on Physics Series (Dover Publications, New York, 1971).
[37] R. S. Christensen, J. Levinsen, and G. M. Bruun, Phys. Rev. Lett. **115**, 160401 (2015).